

## Mechanics of precisely controlled thin film buckling on elastomeric substrate

Hanqing Jiang<sup>a)</sup>

*Department of Mechanical and Aerospace Engineering, Arizona State University, Tempe, Arizona 85287*

Yugang Sun

*Center for Nanoscale Materials, Argonne National Laboratory, 9700 South Cass Avenue, Argonne, Illinois 60439*

John A. Rogers<sup>b)</sup>

*Department of Materials Science and Engineering, Beckman Institute, University of Illinois at Urbana-Champaign, 1304 West Green Street, Urbana, Illinois 61801; Seitz Materials Research Laboratory, University of Illinois at Urbana-Champaign, 1304 West Green Street, Urbana, Illinois 61801; and Department of Mechanical Science and Engineering, University of Illinois at Urbana-Champaign, Urbana, Illinois 61801*

Yonggang Huang

*Department of Mechanical Science and Engineering, University of Illinois at Urbana-Champaign, Urbana, Illinois 61801*

(Received 27 November 2006; accepted 28 February 2007; published online 30 March 2007)

Stretchable electronics has many important and emerging applications. Sun *et al.* [Nature Nanotech. **1**, 201 (2006)] recently demonstrated stretchable electronics based on precisely controlled buckle geometries in GaAs and Si nanoribbons on elastomeric substrates. A nonlinear buckling model is presented in this letter to study the mechanics of this type of thin film/substrate system. An analytical solution is obtained for the buckling geometry (wavelength and amplitude) and the maximum strain in buckled thin film. This solution agrees very well with the experiments, and shows explicitly how buckling can significantly reduce the thin film strain to achieve the system stretchability. © 2007 American Institute of Physics. [DOI: 10.1063/1.2719027]

Stretchable electronics have many important and emerging applications in devices, such as an eyelike digital camera,<sup>1</sup> comfortable skin sensor,<sup>2</sup> intelligent surgical gloves,<sup>3</sup> and structural health monitoring devices.<sup>4</sup> There exist several approaches to fabricate the stretchable electronics. One scenario used stretchable interconnects of metal wires to link electronic components (e.g., transistors) on isolated, rigid islands.<sup>5–10</sup> Another different, but complementary, approach is to produce stretchable components directly based on periodic, sinusoidal wavylike single crystalline Si ribbons on an elastomeric substrate.<sup>11</sup> Field-effect transistors, *p-n* diodes, and other devices for electronic circuits can be directly integrated into the Si to yield fully stretchable components.

The latter approach<sup>11</sup> has the following limitations. (1) The “wavy” Si ribbons are formed from spontaneous buckling with amplitudes and wavelengths determined by material properties (e.g., moduli and thickness), without any direct control over the geometries. (2) Although the range of acceptable strain is improved significantly (to ~20%) compared to that of silicon itself (~1%), the stretchability is still too small for certain applications. In order to control the buckle geometries and improve the stretchability, Sun *et al.*<sup>12</sup> used a mechanical strategy to create precisely controlled buckle geometries for nanoribbons of GaAs and Si, which combines lithographically patterned surface bonding chemistry and a buckling process similar to that reported by Khang *et al.*<sup>11</sup>

As illustrated in Fig. 1, the photolithograph process to define the bonding chemistry is conducted on a stretched poly(dimethylsiloxane) (PDMS) substrate subject to prestrain  $\epsilon_{\text{pre}} = \Delta L/L$  along the ribbon direction to form periodic interfacial patterns with activated sites where the chemical bonding occurs between thin film (GaAs or Si) and PDMS substrate, as well as inactivated sites where there is only weak van der Waals interactions at the interface. The widths of activated and inactivated sites are denoted as  $W_{\text{act}}$  and  $W_{\text{in}}$ , respectively [Fig. 1(a)]. Thin film ribbons oriented parallel to the prestrain direction are attached to the prestrained and patterned PDMS substrate [Fig. 1(b)]. The relaxation of the prestrain  $\epsilon_{\text{pre}}$  in PDMS leads buckling of these ribbons due to the physical separation of the ribbons from the inactivated sites on the PDMS [Fig. 1(c)]. The wavelength of the buckled structures is  $2L_1 = W_{\text{in}}/(1 + \epsilon_{\text{pre}})$ , and its amplitude  $A$  depends on the geometries of the interfacial patterns ( $W_{\text{act}}$  and  $W_{\text{in}}$ ) and the prestrain. Figure 1(d) shows a tilted-view scanning electron microscope (SEM) image of buckled GaAs ribbons on PDMS, in which  $\epsilon_{\text{pre}} = 60\%$ ,  $W_{\text{act}} = 10 \mu\text{m}$ , and  $W_{\text{in}} = 400 \mu\text{m}$ . Details of the experimental procedures and observations were presented elsewhere.<sup>12</sup>

The relation between the geometries of interfacial patterns and the buckling profiles is important to the stretchability of the thin film/substrate system. In this letter, a nonlinear buckling model is presented to study the buckling behavior and to predict the maximum strain in the thin film as a function of interfacial pattern.

The energy method is used to determine the buckling geometry. The thin film is modeled as an elastic nonlinear von Karman beam,<sup>13</sup> which requires (1) the film thickness

<sup>a)</sup>Electronic mail: hanqing.jiang@asu.edu

<sup>b)</sup>Electronic mail: jrogers@uiuc.edu

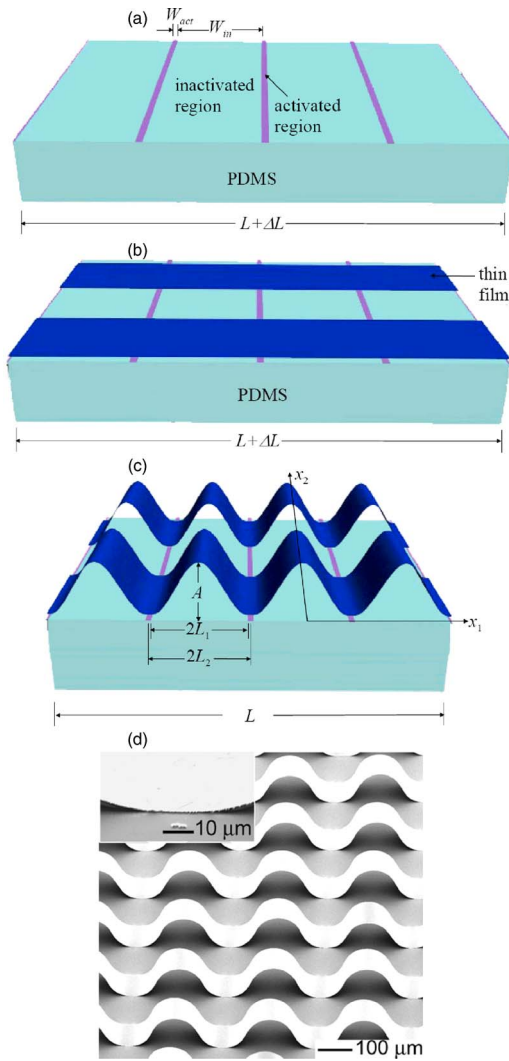


FIG. 1. (Color online) Processing steps for precisely controlled thin film buckling on elastomeric substrate. (a) Prestrained PDMS with periodic activated and inactivated patterns.  $L$  is the original length of PDMS and  $\Delta L$  is the extension. The widths of activated and inactivated sites are denoted as  $W_{act}$  and  $W_{in}$ , respectively. (b) A thin film parallel to the prestrain is attached to the prestrained and patterned PDMS substrate. (c) The relaxation of the prestrain  $\varepsilon_{pre}$  in PDMS leads to buckles of thin film. The wavelength of the buckled film is  $2L_1$  and its amplitude is  $A$ .  $2L_2$  is the sum of activated and inactivated regions after relaxation. (d) Scanning electron microscope (SEM) image of buckled GaAs thin films formed using the previous procedures. The inset shows the GaAs/PDMS substrate interface.

( $\sim 0.1 \mu\text{m}$ ) to be much smaller than any characteristic length in the film plane such as the buckling wavelength ( $\sim 200 \mu\text{m}$ ) and film width and length and (2) the strain in the thin film is negligibly small. The first requirement is always satisfied and the second one to be shown in this letter also holds for this type of thin film/substrate system, which ensures that the von Karman approximation always valid. The PDMS substrate is modeled as a semi-infinite elastic media because its thickness (a few millimeters) is four orders of magnitude larger than the film thickness ( $\sim 0.1 \mu\text{m}$ ). The total energy consists of three parts, the bending energy  $U_b$  due to thin film buckling, membrane energy  $U_m$  in the thin film, and energy  $U_s$  in the substrate. Such an approach was used in prior studies of thin film on elastomeric substrate.<sup>11,14,15</sup>

Upon relaxation of the prestrain in the patterned PDMS, the compressive strain in the thin film induces buckling over

the inactivated (weak bonding) region shown in Fig. 1(d). The buckling profile can be expressed as

$$w = \begin{cases} w_1 = \frac{1}{2}A \left( 1 + \cos \frac{\pi x_1}{L_1} \right), & -L_1 < x_1 < L_1 \\ w_2 = 0, & L_1 < |x_1| < L_2, \end{cases} \quad (1)$$

where  $A$  is the buckling amplitude to be determined,  $x_1$  is the ribbon direction,  $2L_1 = W_{in}/(1 + \varepsilon_{pre})$  is the buckling wavelength, and  $2L_2 = W_{in}/(1 + \varepsilon_{pre}) + W_{act}$  is the sum of activated and inactivated regions after relaxation [Fig. 1(c)]. The bending energy  $U_b$  in the thin film can be obtained from Eq. (1) and the bending rigidity  $h^3 \bar{E}_f / 12$  as  $U_b = \int_{-L_2}^{L_2} 1/2 (h^3 \bar{E}_f / 12) \times (d^2 w / dx_1^2)^2 dx_1 = h^3 \bar{E}_f \pi^4 A^2 / 96 L_1^3$ , where  $h$  is the film thickness,  $\bar{E}_f = E_f / (1 - \nu_f^2)$ ,  $E_f$ , and  $\nu_f$  are the plane-strain modulus, Young's modulus, and Poisson's ratio, respectively.

The membrane strain  $\varepsilon_{11}$ , which determines the membrane energy in the thin film, is related to the displacement  $w$  in Eq. (1) and the in-plane displacement  $u_1$  by  $\varepsilon_{11} = (du_1/dx_1) + (1/2)(dw/dx_1)^2 - \varepsilon_{pre}$ ,<sup>13</sup> where  $-\varepsilon_{pre}$  is the compressive strain due to the relaxation of prestrain  $\varepsilon_{pre}$  in the substrate. Since Young's modulus of PDMS substrate ( $\sim 1 \text{ MPa}$ ) is five orders of magnitude smaller than the Si thin film ( $\sim 100 \text{ GPa}$ ), Huang *et al.*<sup>15</sup> showed that the shear stress at the thin film/substrate interface is negligibly small. The force equilibrium requires a constant membrane force, which gives the in-plane displacement  $u_1 = (A^2 \pi^2 / 4L_1) x_1 (1/3L_2 - 1/4L_1) + (A^2 \pi / 32L_1) \sin(2\pi x_1 / L_1) - \varepsilon_{pre} x_1$  when  $-L_1 < x_1 < L_1$  and  $(A^2 \pi^2 / 12L_1 L_2) x_1 - \varepsilon_{pre} x_1 - (A^2 \pi^2 / 16L_1) \text{sign}(x_1)$  when  $L_1 < |x_1| < L_2$ . The membrane strain then becomes a constant,

$$\varepsilon_{11} = \frac{A^2 \pi^2}{16L_1 L_2} - \varepsilon_{pre}. \quad (2)$$

The membrane energy in the thin film is given by  $U_m = \int_{-L_2}^{L_2} (1/2) h \bar{E}_f \varepsilon_{11}^2 dx_1 = h \bar{E}_f L_2 \varepsilon_{11}^2$ .

The substrate energy  $U_s$  results solely from the displacement/stress traction at the film/substrate interface once the prestrain in the PDMS substrate is relaxed. The long and buckled portion of the thin film ( $2L_1$ ) exerts vanishing stress traction to the substrate directly underneath. The film/substrate interface that remains intact [ $2(L_2 - L_1)$ ] has vanishing displacement, as shown by the SEM image of the GaAs thin film/PDMS substrate interface in the inset of Fig. 1(d), which reveals that the PDMS surface remains flat after relaxation for both activated/inactivated regions. For vanishing displacement and vanishing stress traction, the relaxed PDMS has vanishing energy  $U_s = 0$ .

Minimization of total energy  $\partial U_{tot} / \partial A = 0$  with respect to the buckling amplitude  $A$  gives

$$A = \frac{4}{\pi} \sqrt{L_1 L_2 (\varepsilon_{pre} - \varepsilon_c)} \quad \text{for } \varepsilon_{pre} > \varepsilon_c, \quad (3)$$

where

$$\varepsilon_c = \frac{h^2 \pi^2}{12L_1^2} \quad (4)$$

is the critical strain for buckling, which is identical to the Euler buckling strain for a doubly clamped beam with length  $2L_1$  and bending rigidity  $h^3 \bar{E}_f / 12$ . The thin film does not

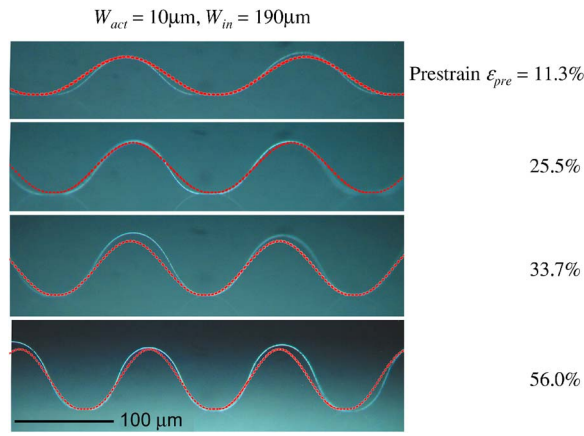


FIG. 2. (Color online) Buckled GaAs thin films on patterned PDMS substrate with  $W_{act}=10\ \mu\text{m}$  and  $W_{in}=190\ \mu\text{m}$  for different prestrain levels, 11.3%, 25.5%, 33.7%, and 56.0% (from top to bottom). The red lines are the profiles of the buckled GaAs thin film predicted by the analytical solution.

buckle when  $\varepsilon_{pre} < \varepsilon_c$ . Once  $\varepsilon_{pre}$  exceeds  $\varepsilon_c$ , the membrane strain obtained from Eqs. (2) and (3) is  $\varepsilon_{11} = -\varepsilon_c$ , i.e., the thin film buckles and adjusts its buckling amplitude  $A$  such that the (compressive) membrane strain remains at  $\varepsilon_c$ .

This analytical solution agrees very well with experiments, as shown in Fig. 2. The red lines are the profiles of the buckled GaAs thin film given by Eqs. (1) and (3) for different prestrain levels with the same layout of interfacial patterns  $W_{act}=10\ \mu\text{m}$  and  $W_{in}=190\ \mu\text{m}$ . The experimental images are also shown for comparison. Good agreement between analytical solutions and experiments is observed for both amplitude and wavelength, except for low prestrain (e.g.,  $\varepsilon_{pre}=11.3\%$ ). This discrepancy is due to the assumption that the thin film buckles over the entire inactivated region, which may not hold at low prestrain.

The critical strain  $\varepsilon_c = h^2 \pi^2 / 12 L_1^2$  in Eq. (4) is on the order of  $10^{-6}$  for the buckling wavelength  $2L_1 \sim 200\ \mu\text{m}$  and thin film thickness  $h \sim 0.1\ \mu\text{m}$ . The buckling amplitude  $A$  in Eq. (3) becomes  $A \approx (4/\pi) \sqrt{L_1 L_2 \varepsilon_{pre}} = (2/\pi) \sqrt{W_{in} [W_{in} + W_{act} (1 + \varepsilon_{pre})] \varepsilon_{pre} / (1 + \varepsilon_{pre})}$ , which is independent of the thin film properties (e.g., thickness, Young's modulus) and is completely determined by the layout of interfacial patterns ( $W_{in}$  and  $W_{act}$ ) and the prestrain. This generic conclusion suggests a broader application of this approach: thin films made of any materials will form into almost the same buckled geometries [shown in Fig. 1(d)] for the same interfacial patterns. Sun *et al.*<sup>12</sup> used this approach to obtain very similar buckled geometries for Si and GaAs.

One of the most important issues in stretchable electronics is to reduce the strain level in electronics. Since the membrane strain  $\varepsilon_{11}$  is negligible ( $\sim 10^{-6}$ ), the maximum strain in the thin film is the bending strain that results from the thin film curvature  $d^2w/dx_1^2$ . This gives

$$\varepsilon_{\max} = \frac{h}{2} \max \left( \frac{d^2w}{dx_1^2} \right) = \frac{h\pi}{L_1^2} \sqrt{L_1 L_2 \varepsilon_{pre}}. \quad (5)$$

For the activated region  $W_{act}$  much smaller than the inactivated region  $W_{in}$ , Eq. (5) can be approximated by  $\varepsilon_{\max} \approx (h\pi/L_1) \sqrt{\varepsilon_{pre}}$ . It is much smaller than the prestrain for thin film thickness  $h$  ( $\sim 0.1\ \mu\text{m}$ ) much less than the wavelength  $2L_1$  ( $\sim 200\ \mu\text{m}$ ). For a  $0.3\ \mu\text{m}$  thin GaAs film buckled on a patterned PDMS substrate with  $W_{act}=10\ \mu\text{m}$ ,  $W_{in}=400\ \mu\text{m}$ , and  $\varepsilon_{pre}=60\%$ , the maximum strain is only 0.6%,

two orders of magnitude smaller than the 60% prestrain. Moreover, this infinitesimal strain (0.6%) ensures that the von Karman beam assumption is always valid in this study. The precisely controlled buckling can significantly reduce the maximum strain in thin film, and improve the system stretchability.

For very long inactivated region, buckling profiles different from Eq. (1) have been observed in experiments. For example, when  $W_{in}=760\ \mu\text{m}$  and  $\varepsilon_{pre}=33.7\%$ , instead of a long wave with wavelength  $2L_1 = W_{in}/(1 + \varepsilon_{pre}) = 568\ \mu\text{m}$  as in Eq. (1), two or three short waves with wavelength about  $100\ \mu\text{m}$  have been observed in experiments. Between the short waves the thin film and substrate remain bonded. The short waves are due to the competition between bending energy and interfacial adhesive energy, which will be further investigated.

The buckled thin films (such as GaAs nanoribbons) need protection in practical applications. This is achieved by embedding the buckled thin films in PDMS (i.e., film sandwiched between PDMS) via the casting and curing of a prepolymer. The prepolymer is fluid which can flow and fill the air gaps between buckled thin film and PDMS substrate.<sup>12</sup> Such a procedure does not change the wavelength ( $2L_1$ ) nor the amplitude ( $A$ ) because the liquid prepolymer does not impose any deformation to the thin film. The stretchability of embedded system will be investigated elsewhere.

One of the authors (H.J.) acknowledges the financial support from the Fulton School of Engineering at ASU. Another author (Y.S.) acknowledges the support of the U.S. Department of Energy, Office of Science, Office of Basic Energy Sciences, under Contract No. DE-AC02-06CH11357. This work was also supported by the Defense Advanced Research Projects Agency-funded Air Force Research Laboratory-managed Microelectronics Program Contract No. FA8650-04-C-7101, by the U.S. Department of Energy under Grant No. DEFG02-91-ER4543, and by NSF under Grant No. DMI-0328162.

<sup>1</sup>H. C. Jin, J. R. Abelson, M. K. Erhardt, and R. G. Nuzzo, *J. Vac. Sci. Technol. B* **22**, 2548 (2004).

<sup>2</sup>V. Lumelsky, M. S. Shur, and S. Wagner, *IEEE Sens. J.* **1**, 41 (2001).

<sup>3</sup>T. Someya, T. Sekitani, S. Iba, Y. Kato, H. Kawaguchi, and T. Sakurai, *Proc. Natl. Acad. Sci. U.S.A.* **101**, 9966 (2004).

<sup>4</sup>A. Nathan, B. Park, A. Sazonov, S. Tao, I. Chan, P. Servati, K. Karim, T. Charania, D. Striakhilev, Q. Ma, and R. V. R. Murthy, *Microelectron. J.* **31**, 883 (2000).

<sup>5</sup>R. Faez, W. A. Gazotti, and M. A. De Paoli, *Polymer* **40**, 5497 (1999).

<sup>6</sup>S. P. Lacour, S. Wagner, Z. Y. Huang, and Z. Suo, *Appl. Phys. Lett.* **82**, 2404 (2003).

<sup>7</sup>D. S. Gray, J. Tien, and C. S. Chen, *Adv. Mater. (Weinheim, Ger.)* **16**, 393 (2004).

<sup>8</sup>C. A. Marquette and L. J. Blum, *Biosens. Bioelectron.* **20**, 197 (2004).

<sup>9</sup>S. P. Lacour, J. Jones, S. Wagner, T. Li, and Z. Suo, *Proc. IEEE* **93**, 1459 (2005).

<sup>10</sup>T. Someya, Y. Kato, T. Sekitani, S. Iba, Y. Noguchi, Y. Murase, H. Kawaguchi, and T. Sakurai, *Proc. Natl. Acad. Sci. U.S.A.* **102**, 12321 (2005).

<sup>11</sup>D. Y. Khang, H. Jiang, Y. Huang, and J. A. Rogers, *Science* **311**, 208 (2006).

<sup>12</sup>Y. Sun, W.-M. Choi, H. Jiang, Y. Huang, and J. A. Rogers, *Nature Nanotech.* **1**, 201 (2006).

<sup>13</sup>S. P. Timoshenko and J. M. Gere, *Theory of Elastic Stability* (McGraw-Hill, New York, 1961).

<sup>14</sup>X. Chen and J. W. Hutchinson, *J. Appl. Mech.* **71**, 597 (2004).

<sup>15</sup>Z. Y. Huang, W. Hong, and Z. Suo, *J. Mech. Phys. Solids* **53**, 2101 (2005).